JOURNAL OF PHYSICAL ORGANIC CHEMISTRY
J. Phys. Org. Chem. 2004; **17:** 724–734
Published online in Wiley InterScience (www.interscience.wiley.com). DOI: 10.1002/poc.787

Synthesis and photochemistry of a carotene–porphyrin–fullerene model photosynthetic reaction center

Gerdenis Kodis, Paul A. Liddell, Ana L. Moore, Thomas A. Moore and Devens Gust*

Department of Chemistry and Biochemistry, Center for the Study of Early Events in Photosynthesis, Arizona State University, Tempe, Arizona 85287, USA

ABSTRACT: A new photosynthetic reaction center mimic consisting of a porphyrin (P) linked to both a fullerene electron acceptor (C_{60}) and a carotenoid secondary electron donor (C) was synthesized and studied in 2-methyltetrahydrofuran using transient spectroscopic methods. Excitation of the porphyrin is followed by photoinduced electron transfer to the fullerene ($\tau = 32$ ps) to yield C–$P^{\cdot+}$–$C_{60}^{\cdot-}$. Electron transfer from the carotene to the porphyrin radical cation ($\tau = 125$ ps) gives a final $C^{\cdot+}$–P–$C_{60}^{\cdot-}$ state with an overall yield of 0.95. This state decays to give the carotenoid triplet state with a time constant of 57 ns. The molecular triad is highly soluble in organic solvents and readily synthesized. These qualities make the molecule a useful artificial photosynthetic reaction center for a variety of spectroscopic and photochemical investigations. Copyright © 2004 John Wiley & Sons, Ltd.

KEYWORDS: carotene; porphyrin; fullerene; photoinduced electron transfer; spectroscopy

INTRODUCTION

Of the large number of porphyrin-based molecules prepared as models for photosynthetic reaction centers, multicomponent 'supermolecules' consisting of three or more electron donor and acceptor units have been shown to be most effective at not only undergoing photoinduced electron transfer to produce an energetic charge-separated state in high quantum yield, but also retarding charge recombination to the ground state.[1–5] Since our report of photoinduced electron transfer in a porphyrin–fullerene dyad in 1994,[6] fullerenes have proven to be excellent electron acceptor moieties for incorporation into such molecules. This is due in part to the low solvent and internal reorganization energies of fullerenes, and the insensitivity of their radical anions to solvent stabilization effects.[7–13]

Carotenoid (C)–porphyrin (P)–fullerene (C_{60}) triad molecules are especially useful models for natural photosynthetic processes.[11–18] Irradiation of these molecules produces the porphyrin first excited singlet state C–^{1}P–C_{60}, which undergoes photoinduced electron transfer to give C–$P^{\cdot+}$–$C_{60}^{\cdot-}$. This initial charge-separated state undergoes charge shift to produce a final, long-lived $C^{\cdot+}$–P–$C_{60}^{\cdot-}$ charge-separated state. Such triads have been shown to demonstrate photoinduced electron transfer in solution and in glassy media at temperatures as low as 8 K to form long-lived charge-separated states whose lifetimes are magnetic field dependent. These states undergo charge recombination to give spin-polarized carotenoid triplet states. They illustrate triplet–triplet energy transfer phenomena related to photosynthetic protection from singlet oxygen damage and singlet–singlet energy transfer related to photosynthetic antenna function. For these reasons, they are excellent candidates for investigation by a wide variety of methods, including ultrafast absorption and emission spectroscopy, magnetic field-dependent techniques,[17] time-resolved EPR spectroscopy in various media[19] and transient d.c. photocurrent methods for dipole moment determination.[20]

We have undertaken the design and synthesis of a C–P–C_{60} triad that is optimized for such investigations. In general, the following characteristics are necessary and/or desirable in such a triad:

i. photoinduced electron transfer on the picosecond time-scale to give C–$P^{\cdot+}$–$C_{60}^{\cdot-}$;
ii. rapid charge shift to produce $C^{\cdot+}$–P–$C_{60}^{\cdot-}$ with a yield approaching unity;
iii. a long-lived $C^{\cdot+}$–P–$C_{60}^{\cdot-}$ state that recombines to yield the carotenoid triplet state, ^{3}C–P–C_{60};
iv. low sensitivity to oxidative damage;
v. high solubility in a variety of solvents;
vi. synthetic accessibility.

Here, we report the synthesis and photochemistry of triad **1**, which fulfills these criteria. The design of **1** draws on experience gained from earlier studies of related triads **2**–**4** (Scheme 1) in order to ensure a high quantum yield of long-lived charge separation. The incorporation of mesityl groups at the 10- and 20-positions of the porphyrin is desirable from a synthetic point of view because

**Correspondence to:* D. Gust, Department of Chemistry and Biochemistry, Arizona State University, Tempe, Arizona 85287, USA.
E-mail: gust@asu.edu
Contract/grant sponsor: National Science Foundation; *Contract/grant numbers:* CHE-0078835, DIR9017262.

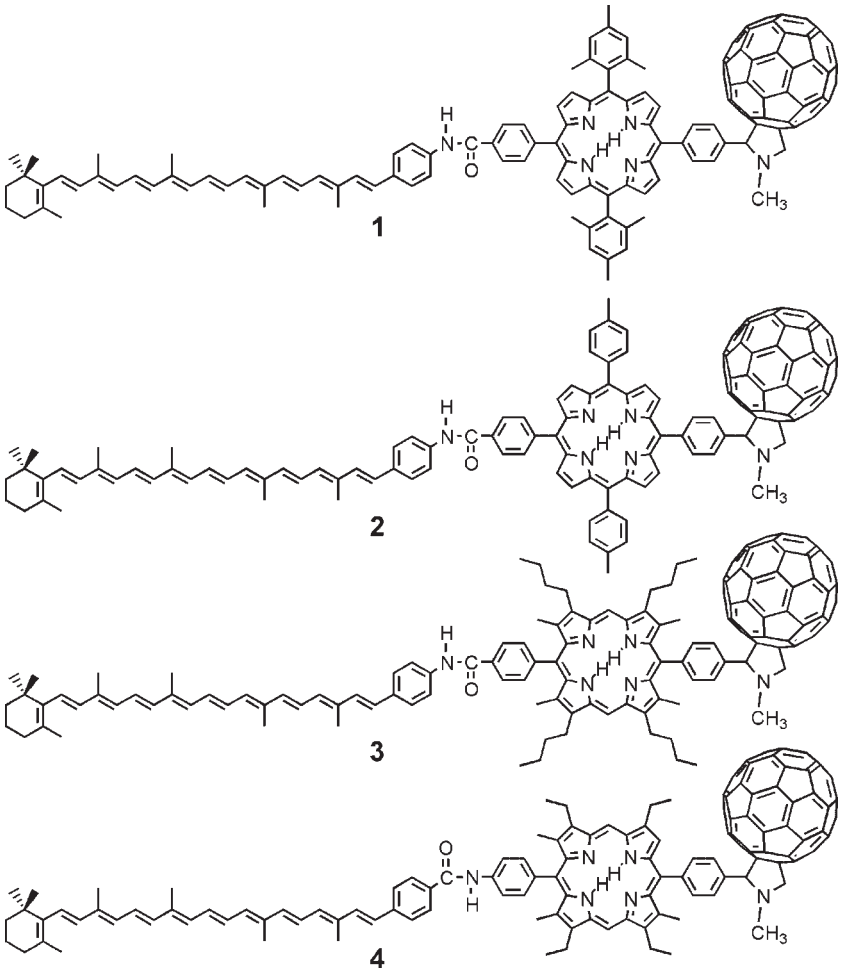

Scheme 1. Structures of carotene–porphyrin–fullerene triad **1** and triads reported earlier (**2**–**4**)

they limit aryl group scrambling during porphyrin preparation.[21] Additionally, these groups increase solubility and limit any tendency of the triads to aggregate.[22]

EXPERIMENTAL

Instrumental techniques

^{1}H NMR spectra were recorded on Varian Unity spectrometers at 300 or 500 MHz. Unless specified otherwise, samples were dissolved in deuterochloroform with tetramethylsilane as an internal reference. High-resolution mass spectra were obtained on a Kratos MS 50 mass spectrometer operating at 8 eV in the fast atom bombardment (FAB) mode. Other mass spectra were obtained on a matrix-assisted laser desorption/ionization time-of-flight (MALDI-TOF) mass spectrometer. Ultraviolet–visible ground-state absorption spectra were measured on a Shimadzu UV2100U UV–VIS spectrometer.

Steady-state fluorescence emission spectra were measured using a Photon Technology International MP-1 spectrometer and corrected for detection system response. Excitation was produced by a 75 W xenon lamp and single-grating monochromator. Fluorescence was detected 90° to the excitation beam via a single grating monochromator and an R928 photomultiplier tube having S-20 spectral response operating in the single photon counting mode.

Fluorescence decay measurements were performed on $\sim 1 \times 10^{-5}$ M solutions by the time-correlated single photon counting method. The excitation source was a cavity-dumped Coherent 700 dye laser pumped by a frequency-doubled Coherent Antares 76s Nd:YAG laser. Fluorescence emission was detected at a magic angle using a single grating monochromator and microchannel plate photomultiplier (Hamamatsu R2809U-11). The instrument response time was ca 35–50 ps, as verified by scattering from Ludox AS-40. The spectrometer was controlled by software based on a LabView program from National Instruments.[23]

Nanosecond transient absorption measurements were made with excitation from an Opotek optical parametric oscillator pumped by the third harmonic of a Continuum Surelight Nd:YAG laser. The pulse width was ~ 5 ns and the repetition rate was 10 Hz. The detection portion of the spectrometer has been described elsewhere.[24]

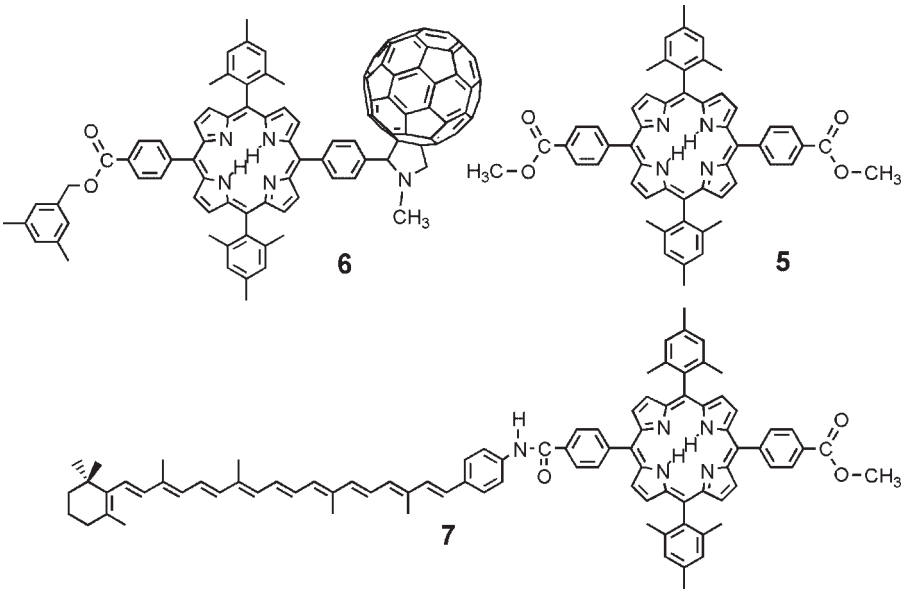

Scheme 2. Structures of model porphyrin **5**, porphyrin–fullerene dyad **6**, and carotenoporphyrin **7**

The femtosecond transient absorption apparatus consists of a kilohertz pulsed laser source and a pump–probe optical setup. The laser pulse train was provided by a Ti:sapphire regenerative amplifier (Clark-MXR, Model CPA-1000) pumped by a diode-pumped continuous-wave solid-state laser (Spectra-Physics, Model Millennia V). The typical laser pulse was 100 fs at 790 nm, with a pulse energy of 0.9 mJ at a repetition rate of 1 kHz. Most of the laser energy (80%) was used to pump an optical parametric amplifier (IR-OPA, Clark-MXR). The excitation pulse was sent through a computer-controlled optical delay line. The remaining laser output (20%) was focused into a 1.2 cm rotating quartz plate to generate a white light continuum. The continuum beam was further split into two identical parts and used as the probe and reference beams, respectively. The probe and reference signals were focused on to two separated optical fiber bundles coupled to a spectrograph (Acton Research, Model SP275). The spectra were acquired on a dual diode-array detector (Princeton Instruments, Model DPDA-1024).[25]

To determine the number of significant components in the transient absorption data, singular value decomposition analysis[26,27] was carried out using locally written software based on the MatLab 5.0 program (MathWorks) Decay-associated spectra were then obtained by fitting the transient absorption change curves over a selected wavelength region simultaneously as described by

$$\Delta A(\lambda, t) = \sum_{i=1}^{n} A_i(\lambda)\exp(-t/\tau_i) \qquad (1)$$

where $\Delta A(\lambda,t)$ is the observed absorption change at a given wavelength at time delay t and n is the number of kinetic components used in the fitting. A plot of $A_i(\lambda)$ versus wavelength is called a decay-associated spectrum, and represents the amplitude spectrum of the ith kinetic component, which has a lifetime of τ_i.

Synthesis

The preparation of porphyrin **5** and porphyrin–fullerene dyad **6** (Scheme 2) has been reported previously.[28]

Carotenoporphyrin–fullerene triad 1. To a flask containing 50 mg (0.033 mmol) of 4-{15-[4-(1′,5′-dihydro-1′-methyl-2′*H*-[5,6]fullereno-C_{60}-I_h-[1,9-*c*]pyrrol-2′-yl)phenyl]-10,20-bis(2,4,6-trimethylphenyl)-21*H*,23*H*-porphin-5-yl}benzoic acid[28] were added 17 mg (0.033 mmol) of 7′-apo-7′-(4-aminophenyl)-β-carotene,[29] 10 ml of pyridine, 1 mg (0.007 mmol) of 4-dimethylaminopyridine and 10 mg (0.049 mmol) of 1-[3-(dimethylamino)propyl]-3-ethylcarbodiimide hydrochloride. The reaction mixture was stirred for 14 h under an argon atmosphere, after which time TLC analysis (dichloromethane) indicated that the reaction was complete. The solvent was distilled at reduced pressure and the residue was chromatographed on a silica gel column (dichloromethane), followed by recrystallization from dichloromethane–hexanes to give 55 mg (83% yield) of triad **1**: ^{1}H NMR (300 MHz, $CDCl_3$), δ −2.64 (2 H, s, NH), 1.03 (6 H, s, car-16,17-CH_3), 1.44 – 1.49 (2 H, m, car-2-CH_2), 1.58–1.66 (2 H, m, car-3-CH_2), 1.72 (3 H, s, car-18-CH_3), 1.81 (6 H, s, Ar-CH_3), 1.83 (6 H, s, Ar-CH_3), 1.98 (3 H, s, car-19-CH_3), 1.99 (3 H, s, car-20-CH_3), 2.01 (3 H, s, car-20′-CH_3), 2.08 (3 H, s, car-19′-CH_3), 2.61 (6 H, s, Ar-CH_3), 3.11 (3 H, s, N-CH_3), 4.43 (1 H, d, $J = 9$ Hz, pyrrolid-H), 5.11 (1 H, d, $J = 9$ Hz, pyrrolid-H), 5.27 (1 H, s, pyrrolid-H), 6.16–6.95 (14 H, m, carotene vinyl H), 7.27 (4 H, s, mesityl-H), 7.52 (2 H, d, $J = 8$ Hz, car-1′,5′-Ar-H), 7.76

(2 H, d, $J = 8$ Hz, car-2′,4′-Ar-H), 8.12 (1 H, s, NH), 8.23–8.43 (8 H, m, Ar-H), 8.67 (4 H, brs, β-H), 8.70 (2 H, d, $J = 5$ Hz, β-H), 8.74 (2 H, d, $J = 5$ Hz, β-H); MALDI-TOFMS, m/z calcd for $C_{151}H_{92}N_6O_1$ 2006, observed 2006; UV–VIS (CH_2Cl_2), 255, 420, 480, 512, 550, 592, 648, 704 nm.

RESULTS AND DISCUSSION

Energetics

The energies of the C–P$^{\cdot+}$–$C_{60}^{\cdot-}$ and C$^{\cdot+}$–P–$C_{60}^{\cdot-}$ charge-separated states may be estimated from cyclic voltammetric measurements on model compounds. In benzonitrile solution containing 0.1 M tetrabutylammonium hexafluorophosphate, the first and second reduction potentials of the fullerene moiety are taken as -0.56 and -0.97 V vs SCE, respectively, whereas the first oxidation potential of the porphyrin moiety is 1.02 V vs SCE.[30] The first oxidation potential of a model carotenoid is 0.47 V vs SCE.[31] Based on these results, C–P$^{\cdot+}$–$C_{60}^{\cdot-}$ and C$^{\cdot+}$–P–$C_{60}^{\cdot-}$ lie approximately 1.58 and 1.03 eV above the ground state, respectively.

Absorption spectra

The absorption spectra of triad **1**, model porphyrin **5** and model P–C_{60} dyad **6** in 2-methyltetrahydrofuran are shown in Fig. 1. The spectra have been normalized at the porphyrin Q-band at 648 nm to facilitate comparison. The bands at ~255 and 705 nm, with continuous weak absorption at intervening wavelengths, are characteristic of fullerene absorption. The carotenoid bands in the triad are observed at 457, 484 and 516 nm, whereas the maxima at 400 (shoulder), 418, 513 (partially obscured by the carotenoid absorption), 547, 592 and 648 nm arise from the porphyrin moiety. It is clear from the figure that the absorption spectrum is essentially a linear combination of the absorption spectra of the component moieties, and there are no significant perturbations that would indicate strong interactions among the linked chromophores. The spectra reveal that it is possible to excite the porphyrin moiety nearly exclusively with irradiation at 650 or 590 nm.

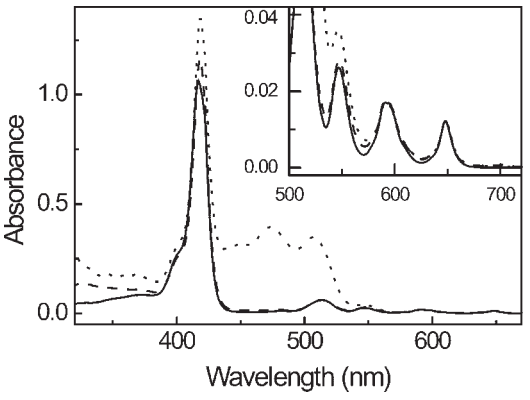

Figure 1. Absorption spectra in 2-methyltetrahydrofuran of triad **1** (···), model dyad **6** (– – –) and model porphyrin **5** (——). The inset is an expansion of the porphyrin Q-band absorption region

Fluorescence emission

The fluorescence emission spectra of **1**, **5**, **6** and **7** in 2-methyltetrahydrofuran solution are shown in Fig. 2. The solutions had identical absorbance at the 590 nm excitation wavelength, where most of the light is absorbed by the porphyrin moiety. Carotenoid polyenes do not fluoresce appreciably, and the emission is due mostly to the porphyrin moiety in all of the spectra. The emission spectra feature maxima at 650 and 718 nm, which are characteristic of free-base tetraarylporphyrins. The ratios of these two peaks in triad **1** and dyad **6** are slightly different from those in **5** and **7**. This is attributed to a small amount of fullerene excitation at 590 nm, with consequent fullerene emission around 715 nm; the effect is not observed with excitation at 650 nm.

The porphyrin fluorescence of carotenoporphyrin dyad **7** is slightly quenched relative to that of the porphyrin alone. Such quenching has been observed in other carotenoporphyrins, and in some cases is due to photoinduced electron transfer from the carotenoid to the porphyrin.[22,32–36] From the results for triad **1** and dyad **6**, it is evident that attachment of the fullerene moiety to the porphyrin leads to much more substantial quenching. In earlier work on C–P–C_{60} triads, this has been shown to be due to photoinduced electron transfer to form a C–P$^{\cdot+}$–$C_{60}^{\cdot-}$ charge-separated state.[11–18]

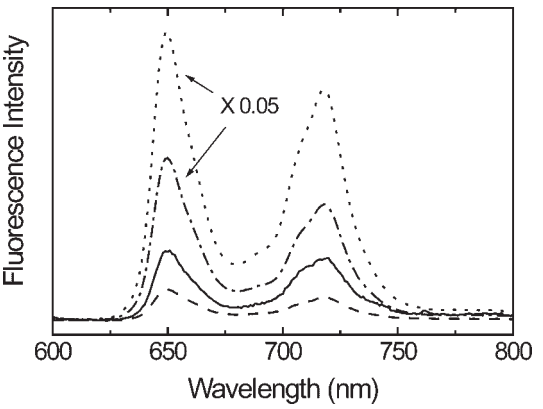

Figure 2. Fluorescence emission spectra in 2-methyltetrahydrofuran solution of triad **1** (——), model dyad **6** (– – –), model porphyrin **5** (···) and carotenoporphyrin dyad **7** (– · –), with excitation at 590 nm, where the porphyrin moiety absorbs most of the light. All samples had the same optical density at 590 nm. Note that the fluorescence intensities of **5** and **7** have been multiplied by 0.05 in order to facilitate comparison

Time-resolved fluorescence

In situations of strong fluorescence quenching, such as for triad **1** and dyad **6**, steady-state fluorescence intensities are difficult to employ for determination of quenching rate constants because a tiny amount of highly fluorescent impurity (e.g. porphyrin) can dominate the observed fluorescence. For this reason, we undertook a time-resolved study of the fluorescence of **1** and its model compounds in 2-methyltetrahydrofuran using the single photon timing technique. Solutions of triad **1**, model porphyrin **5** and dyads **6** and **7** were excited at 590 nm, and the fluorescence decays were measured at five wavelengths in the 630–820 nm range. Analysis of the data for model porphyrin **5** yielded a single exponential decay with a lifetime of 10.2 ns ($\chi^2 = 1.19$). Analysis of the data for dyad **6** ($\chi^2 = 1.16$) yielded one significant decay component with a lifetime of 34 ps and three minor ($\leq$5% of the decay) components with lifetimes of 0.25, 1.7 and 8.8 ns. The minor components are ascribed to a small amount of impurity. The slight quenching observed in the steady-state experiments on carotenoporphyrin **7** is also observed in the time-resolved experiments. A lifetime of 4.7 ns ($\chi^2 = 1.12$) for the porphyrin first excited singlet state of **7** was measured. In the case of triad **1**, the results are very similar to those obtained for porphyrin–fullerene dyad **6**. One significant decay component with a lifetime of 34 ps was noted ($\chi^2 = 1.09$), accompanied by minor ($\leq$5% of the decay) components of 0.19, 1.7 and 4.9 ns. The significant shortening of the porphyrin excited-state lifetimes in **1** and **6** relative to those of the corresponding states in **5** and **7** is ascribed to photoinduced electron transfer to the fullerene moiety, as also suggested by the steady-state emission spectra discussed above.

Time-resolved absorption

Transient absorption experiments were undertaken in order to quantify better the interconversions of the various excited states in these compounds and to allow the detection of charge-separated species and other non-emissive states. Solutions of **1** and **6** in 2-methyltetrahydrofuran were excited with ~100 fs laser pulses and the transient absorption was recorded using the pump–probe method (see Experimental section). The samples were excited in the porphyrin Q-band absorbance at 600 nm and the spectra were recorded in the 930–1070 and 450–760 nm regions. For triad **1**, 70 kinetic traces were measured over those wavelength regions, at times ranging from −50 to 4500 ps relative to the laser flash. For dyad **6**, 155 kinetic traces were determined over the same time range. The data obtained were fitted globally using singular value decomposition methods.

Results for dyad **6** are presented in Fig. 3. The inset shows the transient absorption in the near-infrared region

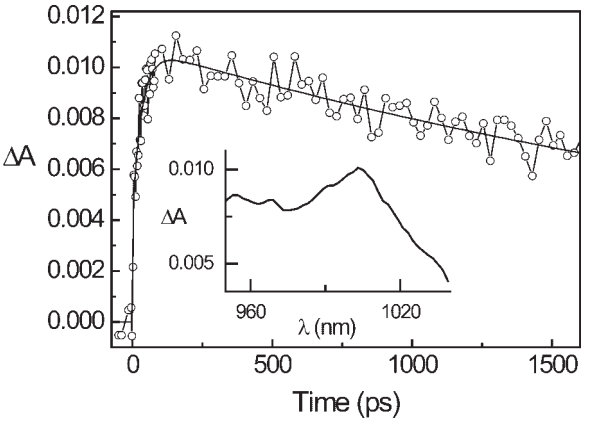

Figure 3. Transient absorption kinetics measured at 1000 nm in 2-methyltetrahydrofuran for dyad **6** with excitation at 600 nm with an ~100 fs laser pulse. The smooth line results from a global analysis of the data at all wavelengths and features a rise time of 32 ps and a decay time constant of 3.3 ns. The inset shows the transient absorption of the $P^{\cdot+}$–$C_{60}^{\cdot-}$ charge-separated state taken 500 ps after excitation

500 ps after laser excitation. The absorption maximum at around 1000 nm is characteristic of the fullerene radical anion, and verifies formation of the $P^{\cdot+}$–$C_{60}^{\cdot-}$ charge-separated state. The complementary very broad porphyrin radical cation absorption in the visible optical region was also observed, and follows the same kinetics. Figure 3 shows kinetics determined at 1000 nm. The fullerene radical anion absorption rises with a time constant of 32 ps, which is therefore the formation time constant for $P^{\cdot+}$–$C_{60}^{\cdot-}$. The charge-separated state decays to the ground state with a lifetime of 3.3 ns.

Similar experiments were carried out with triad **1** (Fig. 4). Figure 4(a) shows a typical kinetic trace, taken at 980 nm. Figure 4(b) shows decay-associated spectra (600–800 nm region) of **1** obtained by a global analysis of all of the data. The best fit was obtained with three exponential components: 30 ps, 120 ps and a component that does not decay on this time-scale. The spectrum of the 30 ps component has negative bands due to ground-state bleaching of the porphyrin at ~650 nm and porphyrin stimulated emission around 725 nm. Hence, it represents the decay of the porphyrin first excited singlet state C–^{1}P–C_{60} and formation of C–$P^{\cdot+}$–$C_{60}^{\cdot-}$. The 120 ps component shows negative amplitude at ~590 and ~650 nm and in the 700 nm region. This indicates a disappearance of ground-state bleaching of the porphyrin radical cation (decay of the C–$P^{\cdot+}$–$C_{60}^{\cdot-}$ state) and a rise of broad induced absorption due to the edge of the carotenoid radical cation absorption (formation of $C^{\cdot+}$–P–$C_{60}^{\cdot-}$). The $C^{\cdot+}$–P–$C_{60}^{\cdot-}$ state has characteristically strong absorption in the 950–1000 nm region due to the carotenoid radical cation (centered at ~980 nm) and fullerene radical anion [see inset in Fig. 4(a)]. The non-decaying component of the decay-associated spectrum is dominated by the tail of the broad

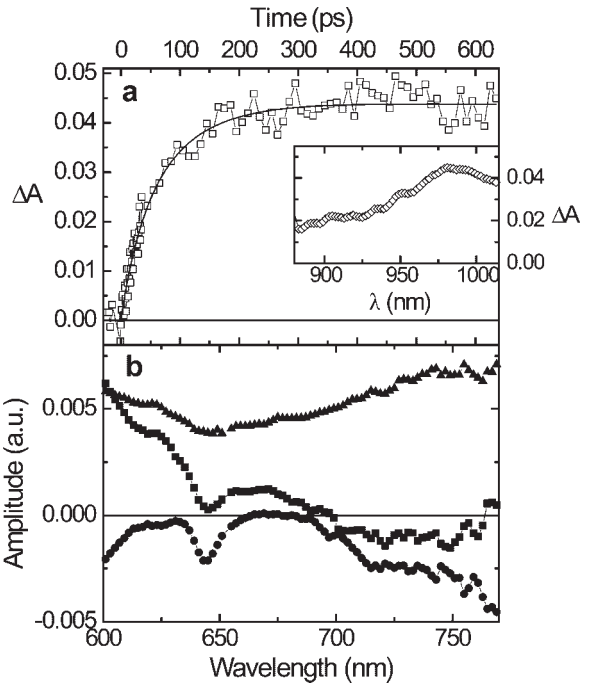

Figure 4. (a) Transient absorption kinetics measured at 980 nm for triad **1** in 2-methyltetrahydrofuran, following excitation at 600 nm with an ~100 fs laser pulse. The smooth curve is a three-exponential fit to the data with time constants of 30 ps, 120 ps and a non-decaying component. The inset shows the transient absorption spectrum measured 3 ns after excitation. (b) Decay-associated spectra for **1** in 2-methyltetrahydrofuran obtained from a global analysis of transient absorption data taken after excitation at 600 nm. The lifetimes of the components are 30 ps (■), 120 ps (●) and non-decaying (▲)

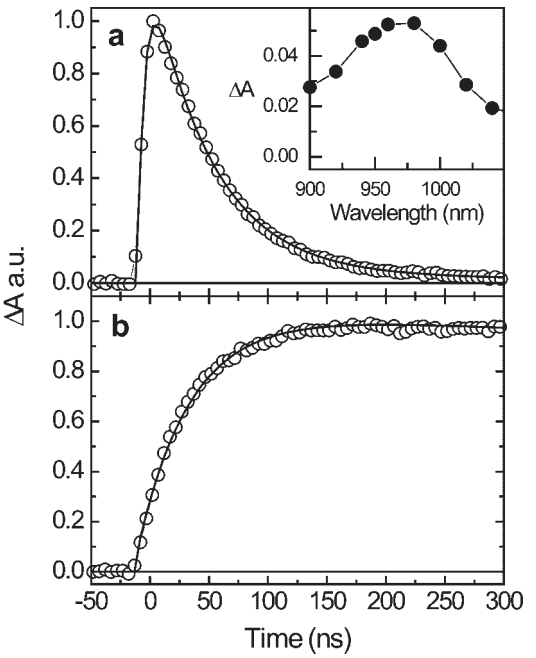

Figure 5. Transient absorption kinetics measured for triad **1** in deoxygenated 2-methyltetrahydrofuran following excitation at 600 nm with a 5 ns laser pulse. (a) Kinetic trace at 980 nm. An exponential fit to the data with a time constant of 57 ns is shown as a smooth curve. The inset shows the transient absorption spectra measured 50 ns after excitation. (b) Kinetic trace at 550 nm. A two-exponential fit to the data with time constants of 57 ns and 4.9 μs is shown as a smooth curve

induced absorption due to the carotenoid radical cation, and does not contain porphyrin features.

The time-scale of the transient absorption experiments discussed above is too short to allow observation of the decay of the $C^{\cdot+}$–P–$C_{60}^{\cdot-}$ state. Therefore, transient absorption spectroscopy on the nanosecond time-scale was employed for investigation of the long-lived state. Figure 5 shows some results of these experiments, which employed 600 nm excitation of a deoxygenated 2-methyltetrahydrofuran solution of **1** with a 5 ns laser pulse. The inset in Fig. 5(a) shows the spectrum of $C^{\cdot+}$–P–$C_{60}^{\cdot-}$, with a maximum at ~980 nm, taken 50 ns after excitation. The decay of this absorption is shown in Fig. 5(a), along with an exponential fit with a time constant of 57 ns. The decay of $C^{\cdot+}$–P–$C_{60}^{\cdot-}$ is accompanied by a complementary exponential rise of the absorbance at 550 nm with a 57 ns time constant [Fig. 5(b)]. Absorbance at this wavelength is due to the carotenoid triplet state, and its rise indicates the formation of ^{3}C–P–C_{60} by charge recombination of $C^{\cdot+}$–P–$C_{60}^{\cdot-}$. The decay of this absorbance can be observed on an even longer time-scale, and has a time constant of 4.9 μs in the absence of oxygen. The lifetime is oxygen sensitive.

The quantum yield of $C^{\cdot+}$–P–$C_{60}^{\cdot-}$ was estimated by the comparative method.[37] This was done by comparing the amplitude of the carotenoid radical cation absorbance at its maximum with that of a related C–P–C_{60} triad having a yield of 0.88 for the $C^{\cdot+}$–P–$C_{60}^{\cdot-}$ state.[12] The yield determined in this way was 1.0. The yield of the carotenoid triplet state resulting from charge recombination of $C^{\cdot+}$–P–$C_{60}^{\cdot-}$ was also found to be 1.0 relative to the amount of $C^{\cdot+}$–P–$C_{60}^{\cdot-}$ initially present by comparing the transient absorbance of the carotenoid triplet in **1** with that of the carotenoid radical cation, as described previously.[12]

Discussion

Interpretation of the kinetic data. The spectroscopic results for **1** and the related model compounds may be discussed in terms of Fig. 6, which shows the transient states of **1** and relevant interconversion pathways. The porphyrin first excited singlet state is 1.91 eV above the ground state, based on the wavenumber average of the longest wavelength absorption and shortest wavelength emission maxima. The fullerene first excited singlet state lies at 1.75 eV, but it was not significantly populated during the experiments discussed here. The

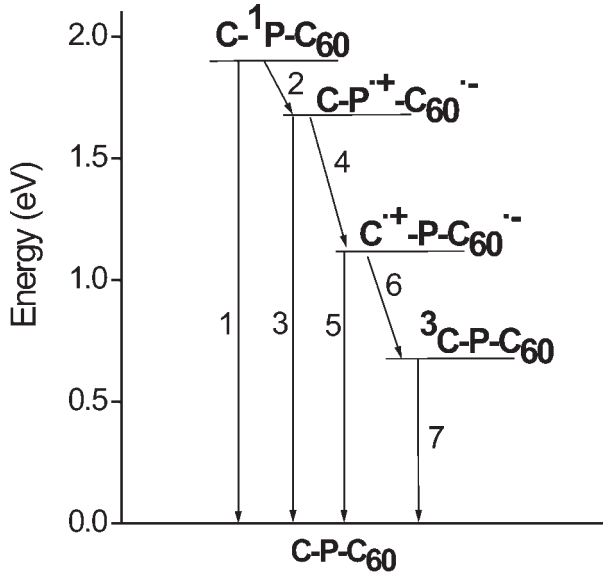

Figure 6. Transient states of triad **1** and relevant interconversion pathways. Each reaction step (1, etc.) has an associated rate constant (k_1, etc.) that is discussed in the text

C–P$^{\cdot+}$–C$_{60}^{\cdot-}$ and C$^{\cdot+}$–P–C$_{60}^{\cdot-}$ charge-separated states are ca 1.58 and 1.03 eV above the ground state, respectively, based on the electrochemical results for model compounds discussed above. No correction for coulombic effects in different solvents has been attempted.

Excitation of the porphyrin moiety of **1** to produce C–^{1}P–C$_{60}$ is followed by photoinduced electron transfer to yield C–P$^{\cdot+}$–C$_{60}^{\cdot-}$ (step 2 in Fig. 6). Although singlet–singlet energy transfer to the fullerene to yield C–P–^{1}C$_{60}$ could in principle compete with electron transfer, no evidence for a rise of the fullerene first excited singlet state was observed in these compounds, or in related ones in polar solvents.[11–17] Hence, the value of k_1 is given by the equation

$$1/\tau_s = k_1 + k_2 \qquad (2)$$

where τ_s is 32 ps, taken as the average of the lifetimes measured by time-resolved emission and absorption techniques. The value of k_1, which is the sum of the rate constants for decay of C–^{1}P–C$_{60}$ by fluorescence, intersystem crossing, internal conversion and carotenoid quenching, may be estimated as $2.1 \times 10^8\ s^{-1}$ from the 4.7 ns lifetime of the porphyrin first excited singlet state in carotenoporphyrin **7**. Hence $k_2 = 3.1 \times 10^{10}\ s^{-1}$. The same value for the photoinduced electron transfer rate constant, within experimental error, may be estimated from the results for porphyrin–fullerene dyad **6**, which had similar decay times for the porphyrin first excited singlet state. The quantum yield of photoinduced electron transfer in **1**, Φ_2, is

$$\Phi_2 = \frac{k_2}{k_1 + k_2} \qquad (3)$$

and equals 0.99.

The C–P$^{\cdot+}$–C$_{60}^{\cdot-}$ state evolves by charge shift step 4, which must compete with charge recombination step 3. The value of k_3 may be estimated from the lifetime of 3.3 ns measured for decay of P$^{\cdot+}$–C$_{60}^{\cdot-}$ in dyad **6**, and equals $3.0 \times 10^8\ s^{-1}$. In triad **1**, the sum of k_3 and k_4 equals the reciprocal of the 120 ps decay time of C–P$^{\cdot+}$–C$_{60}^{\cdot-}$ and concurrent rise time for C$^{\cdot+}$–P–C$_{60}^{\cdot-}$ as measured by transient absorption spectrometry. Thus, $k_4 = 8.0 \times 10^9\ s^{-1}$. The overall quantum yield of the final C$^{\cdot+}$–P–C$_{60}^{\cdot-}$ state, Φ_{fin}, is given by

$$\Phi_{fin} = \Phi_2[k_4/(k_3 + k_4)] \qquad (4)$$

and equals 0.95. This kinetically determined value is within experimental error of the quantum yield of 1.0 determined by the comparative method as discussed above.

Decay of C$^{\cdot+}$–P–C$_{60}^{\cdot-}$ occurs with a time constant of 57 ns, as revealed by the nanosecond transient absorption experiments. The yield of ^{3}C–P–C$_{60}$ was determined to be essentially quantitative, based on the amount of C$^{\cdot+}$–P–C$_{60}^{\cdot-}$. Thus, the only significant decay pathway for C$^{\cdot+}$–P–C$_{60}^{\cdot-}$ is step 6 in Fig. 6, and $k_6 = 1.8 \times 10^7\ s^{-1}$. The ^{3}C–P–C$_{60}$ decays in 4.9 μs, and so $k_7 = 2.0 \times 10^5\ s^{-1}$.

Comparison with other triads. It is clear from the above that triad **1** not only undergoes ultrafast photoinduced electron transfer to give the initial charge-separated state in high yield, but also exhibits a rapid charge shift which competes well with charge recombination of C–P$^{\cdot+}$–C$_{60}^{\cdot-}$ to yield the final C$^{\cdot+}$–P–C$_{60}^{\cdot-}$ state with a quantum yield near unity. The C$^{\cdot+}$–P–C$_{60}^{\cdot-}$ state recombines to yield the carotenoid triplet state, rather than the ground state. Hence **1** is an excellent mimic of some facets of natural photosynthetic reaction center function. Natural reaction centers also produce long-lived charge-separated states with near-unity quantum yield and, under some conditions, recombination of these states to yield chlorophyll or carotenoid triplet states is observed.[38–43] It is of interest to compare the photochemistry of **1** with that of previously reported triads **2**–**4**. Table 1 shows relevant rate constants and quantum yields for these triads in 2-methyltetrahydrofuran at ambient temperatures.

Let us first contrast the photoinduced electron transfer behavior of triad **1**, which features a *meso*-tetraarylporphyrin, with those of **3** and **4**, which are based on diaryloctaalkylporphyrins. Table 1 shows that the initial photoinduced electron transfer from C–^{1}P–C$_{60}$ to yield C–P$^{\cdot+}$–C$_{60}^{\cdot-}$ in **1** (step 2 in Fig. 6) is significantly slower than the corresponding step in triads **3** and **4**. As with most electron-transfer processes, the rate constant for this step is expected to be a function of both the thermodynamic driving force and the electronic coupling between the initial and final states. Looking first at driving force considerations, spectroscopic and cyclic voltammetric measurements in polar solvents allow estimates for the driving force for photoinduced electron transfer from C–^{1}P–C$_{60}$ to yield C–P$^{\cdot+}$–C$_{60}^{\cdot-}$ in triads **1**, **3** and **4**

Table 1. Rate constants[a] ($\times 10^{-8}$) and quantum yields[a] for triads **1**–**4** in 2-methyltetrahydrofuran at 292 K

Compound	k_2 (s^{-1})	k_3 (s^{-1})	k_4 (s^{-1})	k_6 (s^{-1})	$\Phi(C–P^{\cdot+}–C_{60}^{\cdot-})$	$\Phi(C^{\cdot+}–P–C_{60}^{\cdot-})$	$\Phi(^3C–P–C_{60})$
1	310	3.0	80	0.18	0.99	0.95	0.95
2	270	4.8	~290	0.17	0.97	≥0.96	≥0.96
3	3300	21	150	0.029	1.0	0.88	0.88
4	≤1000[b]	110[c]	31[c]	0.059	1.0	0.22[c]	0.22[c]

[a] See Fig. 6 for a diagram showing the processes represented by these quantities.
[b] The value given is an upper limit for k_2.[13]
[c] These values are based on the assumption that the extinction coefficient of the carotenoid radical cation moiety of **4** is identical with that of the corresponding moieties in **2** and **3**.[12]

of 0.33, 0.53 and 0.58 eV, respectively. The difference is due to the fact that the first oxidation potential of tetraarylporphyrins such as that in **1** is typically higher than that for octaalkylporphyrins such as those in **3** and **4**. As step 2 in Fig. 6 undoubtedly occurs in the normal region of the Marcus–Hush electron transfer theory,[44–47] the thermodynamic argument would suggest that the rate constant for step 2 in triad **1** should be substantially smaller that those for the corresponding process in **3** and **4**, and this is in fact observed.

There are also differences in electronic coupling among the molecules. Electronic interaction between the porphyrin donor and fullerene acceptor involves the bonds of the chemical linkage joining them. Part of this coupling is due to the overlap of the π-electron system of the porphyrin with that of the *meso* aryl ring. These two π-systems are not coplanar because of steric hindrance between the aryl *ortho* hydrogens and the β-pyrrole positions on the macrocycle. In porphyrins with no β-substituents and no *ortho* substituents on the phenyl rings involved in donor–acceptor interactions, such as **1**, the aryl rings make angles $\geq 45^\circ$ but $<90^\circ$ with the mean porphyrin ring plane. When β-substituents are present, as in **3** and **4**, the aryl rings are forced into more orthogonal conformations and coupling is reduced.[48,49] Hence steric arguments alone predict more rapid photoinduced electron transfer in **1** than in **3** and **4**.

In addition, the nature of the frontier molecular orbitals on the porphyrin may differ in **1**, relative to **3** and **4**. Porphyrins with eight β-alkyl substituents, such as those in **3** and **4**, are believed to have a_{1u} HOMOs, whereas those lacking the β-substituents have a_{2u} HOMOs. The a_{1u} orbital has nodes at the *meso* positions, whereas the a_{2u} has lobes at the *meso* positions. This difference has been used to explain the fact that *meso*-linked porphyrin arrays with a_{2u} HOMOs undergo singlet–singlet energy transfer by a through-bond mechanism with substantially larger rate constants than *meso*-linked arrays with a_{1u} orbitals.[50–54] Enhanced electronic coupling would also be expected to affect electron-transfer rate constants. Therefore, the orbital ordering would also favor enhanced photoinduced electron transfer in **1**, relative to **3** and **4**. The experimental result, more rapid transfer in **3** and **4** than in **1**, argues that the thermodynamic factors predominate over the steric and electronic effects.

In the triads, the rate constants for photoinduced electron transfer from $C–^1P–C_{60}$ vary by over an order of magnitude, but the quantum yield of formation of $C–P^{\cdot+}–C_{60}^{\cdot-}$ is still essentially unity for all of the molecules because competing processes are much slower. The disparity in yields of the final $C^{\cdot+}–P–C_{60}^{\cdot-}$ species is due to differences in partitioning of $C–P^{\cdot+}–C_{60}^{\cdot-}$ between charge recombination (step 3) and the charge shift reaction (step 4). Again, the rates of these reactions are expected to be a function of thermodynamic driving force and electronic coupling. In **1**, the higher oxidation potential of the porphyrin moiety relative to those of **3** and **4** serves to increase the driving force for both charge recombination and charge shift. With respect to charge recombination reaction step 3, the charge-separated state in **1** lies 1.58 eV above the ground state, whereas the $C–P^{\cdot+}–C_{60}^{\cdot-}$ states of **3** and **4** are ca 0.15 eV lower in energy than that of **1**. At such energies, step 3 is almost certain to lie in the inverted region of the Marcus–Hush relationship, where an increase in driving force leads to a *decrease* in electron transfer rate constant. Table 1 shows that charge recombination of $C–P^{\cdot+}–C_{60}^{\cdot-}$ is indeed significantly slower in triad **1** than in **3** and **4**. The steric and electronic factors discussed above suggest that electronic coupling in **1** could be larger than in **3** and **4**. If this is the case, then the thermodynamic factor again predominates in the charge recombination reaction step 3.

Of course, the yield of $C^{\cdot+}–P–C_{60}^{\cdot-}$ depends not on the absolute rates of steps 3 and 4, but rather on the ratio of rate constants. The thermodynamic driving force for the charge shift reaction (step 4) in **1** is larger than it is for **3** and **4**. The first oxidation potential of the porphyrin of **1** is ca 0.15 V higher than those for the porphyrin moieties of **3** and **4**, and the first oxidation potential of the carotenoid moiety of **4** is ca 0.18 V higher than that for the carotenoid in **1**. If the charge shift reaction occurs in the normal region of the Marcus–Hush relationship, the enhanced driving force for charge shift in **1** should lead to a larger rate constant for the reaction. In addition, to the extent that the electronic coupling is stronger for **1** than for **3** and **4**, the reaction should be more rapid for **1**. Indeed, k_4 appears to be larger for **1** than it is for triad **4** (see Table 1 and its footnotes). However, the rate constant for **1** is slightly smaller than it is in triad **3**. It is dangerous to put too much significance on this comparison, as the difference in rate constants is less than a factor of 2, and

temperatures were not strictly controlled during the determinations. However, it is interesting to speculate on the reasons for the phenomenon. The effect is in accord with Marcus–Hush theory if the charge shift reaction occurs near the point where the driving force $-\Delta G^\circ = \lambda$ (the total reorganization energy for electron transfer), so that in **1**, charge shift, with a driving force of ca 0.55 eV, occurs in the inverted region, and therefore slows relative to the same step in **3**. However, at this time, additional evidence for this interpretation is lacking. In any case, the structural and electronic differences among the molecules produce a ratio k_4/k_3 of 27 for **1**, 7.1 for **3** and 0.28 for **4**. This is the reason for the enhanced quantum yield of $C^{\cdot+}$–P–$C_{60}^{\cdot-}$ in **1** relative to the other two triads.

Electronic coupling and thermodynamic effects are expected to be very similar for triads **1** and **2**, both of which feature *meso*-tetraarylporphyrin chromophores. Replacing a *p*-tolyl group (as in **2**) with a mesityl group (as in **1**) only decreases the oxidation potential of a porphyrin by ca 0.01 V.[55,56] The data in Table 1 show that the photochemistry of the two molecules is indeed very similar. The only significant difference appears to be in the magnitude of k_4, the rate constant for the charge shift reaction. In the case of triad **2**, the somewhat more primitive spectroscopic methods and lower signal-to-noise ratio employed in that study did not permit unambiguous observation of the kinetics of the formation of $C^{\cdot+}$–P–$C_{60}^{\cdot-}$ from C–$P^{\cdot+}$–$C_{60}^{\cdot-}$, and the spectroscopic signatures of the rise times of the two species were convoluted together.[11] Hence the value for k_4 in triad **2** reported in Table 1 is likely somewhat imprecise, and the difference in behavior of **1** and **2** may be less than suggested by the table.

Turning to the charge recombination of the final $C^{\cdot+}$–P–$C_{60}^{\cdot-}$ state to yield ^{3}C–P–C_{60}, it is apparent that recombination is much more rapid for **1** and **2** than for **3** and **4**. In principle, this recombination could occur in a single kinetic step, or could involve a two-step mechanism with an intermediate in which the porphyrin bears a charge. Experiments on **2**–**4** have previously ruled out the two-step mechanism for these triads,[11] although it has been observed in some other kinds of triad molecules.[57,58] Given the one-step mechanism, the slower recombination in triad **3** relative to **4** may be ascribed to the fact that the driving force for recombination is greater in **4**, owing to the higher oxidation potential of the carotenoid (assuming that the triplet state energies in the two carotenoid moieties are similar). Recombination in **1** and **2** is substantially more rapid than in **3**, even though all three triads feature identical carotenoid and fullerene units. Therefore, the difference cannot be due to thermodynamic or structural differences in these moieties. Marcus–Hush theory suggests that the difference in rate constants must be due to differences in electronic coupling. Because the distances between the carotene and fullerene units must be essentially identical for the three molecules, we ascribe the rate constant difference to differences in superexchange electronic coupling via the central porphyrin moiety. As discussed above, steric and electronic factors suggest that such coupling would be stronger for the tetraarylporphyrin-based triads **1** and **2** than for octaalkylporphyrin **3**. The observed differences in recombination rate constants are consistent with this idea.

Recombination of $C^{\cdot+}$–P–$C_{60}^{\cdot-}$ to give the ground state is not observed in any of the four triads in 2-methyltetrahydrofuran. In very polar solvents such as benzonitrile, recombination to give at least some ground state was observed for triads **2** and **3**, but only recombination to the carotenoid triplet state was observed in less polar solvents. EPR and magnetic field effect studies have shown that in the absence of an external magnetic field, $C^{\cdot+}$–P–$C_{60}^{\cdot-}$ exists as a mixture of rapidly equilibrating singlet and triplet biradical states.[17,19] In non-polar solvents, the thermodynamic driving force for recombination to give the carotenoid triplet state is relatively small, and recombination occurs in the normal region of the Marcus–Hush relationship. The driving force for recombination to the ground state is much larger (ca 1 eV), and this reaction likely occurs in the inverted region. Hence the reaction is slow, relative to triplet formation. There is also a statistical preference for triplet formation, because the population of $C^{\cdot+}$–P–$C_{60}^{\cdot-}$ is spread over one singlet biradical and three triplet biradical states.

The photochemical properties of triads **1** and **2** are nearly identical, as expected from the structural similarity. There are, however, other advantages to triad **1** as a photosynthetic mimic. The porphyrin moieties of these molecules are prepared using a method developed by Lee and Lindsay[22] in which a dipyrromethane bearing an aryl substituent is condensed with 4-carbomethoxybenzaldehyde. One complication of this type of reaction is that some scrambling of the aryl groups can occur, leading to the necessity of separating complex mixtures, and a lower yield of the desired porphyrin. The mesityl groups employed in the dipyrromethane used to prepare **1** have been shown to have a much smaller tendency to undergo this ligand scrambling reaction than phenyl groups lacking the *ortho* substituents.[21] This considerably facilitates the synthesis of **1**. In addition, some photochemical and spectroscopic studies require a relatively high solubility for the triad and model compounds in organic solvents, liquid crystals or lipid bilayers. Mesityl-bearing porphyrins have been demonstrated to be significantly more soluble than porphyrins bearing less highly substituted aryl rings.[22]

CONCLUSIONS

Triad **1** has been found to undergo photoinduced electron transfer followed by charge shift to generate the $C^{\cdot+}$–P–$C_{60}^{\cdot-}$ charge-separated state with an overall yield

approaching unity. The state stores about 1.0 eV of the photon energy as electrochemical potential, decaying with a time constant of 57 ns. Recombination yields the carotenoid triplet state, rather than the ground state. This combination of a high yield of energetic, long-lived charge separation and charge recombination to the triplet state is reminiscent of the behavior of photosynthetic reaction centers, and makes **1** a useful model compound for a variety of spectroscopic and photochemical studies. The synthesis of **1** is relatively facile, and it has high solubility in many organic solvents owing to the substitution pattern of the porphyrin aryl groups.

Acknowledgments

This work was supported by the National Science Foundation (CHE-0078835). FAB mass spectrometric studies were performed by the Midwest Center for Mass Spectrometry, with partial support by the National Science Foundation (DIR9017262). This is publication 591 from the ASU Center for the Study of Early Events in Photosynthesis.

REFERENCES

1. Gust D, Mathis P, Moore AL, Liddell PA, Nemeth GA, Lehman WR, Moore TA, Bensasson RV, Land EJ, Chachaty C. *Photochem. Photobiol.* 1983; **37S**: S46.
2. Moore TA, Gust D, Mathis P, Mialocq J-C, Chachaty C, Bensasson RV, Land EJ, Doizi D, Liddell PA, Lehman WR, Nemeth GA, Moore AL. *Nature (London)* 1984; **307**: 630–632.
3. Nishitani S, Kurata N, Sakata Y, Misumi S, Karen A, Okada T, Mataga N. *J. Am. Chem. Soc.* 1983; **105**: 7771–7772.
4. Gust D, Moore TA. In *The Porphyrin Handbook*, Kadish KM, Smith KM, Guilard R (eds). Academic Press: New York, 2000; 153–190.
5. Gust D, Moore AL, Moore TA. In *Electron Transfer in Chemistry: Biological and Artificial Supramolecular Systems*, Vol. 3, Balzani V (ed). Wiley-VCH: Weinheim, 2001; 272–336.
6. Liddell PA, Sumida JP, Macpherson AN, Noss L, Seely GR, Clark KN, Moore AL, Moore TA, Gust D. *Photochem. Photobiol.* 1994; **60**: 537–541.
7. Imahori H, Hagiwara K, Aoki M, Akiyama T, Taniguchi S, Okada T, Shirakawa M, Sakata Y. *J. Am. Chem. Soc.* 1996; **118**: 11771–11782.
8. Imahori H, Hagiwara K, Akiyama T, Aoki M, Taniguchi S, Okada T, Shirakawa M, Sakata Y. *Chem. Phys. Lett.* 1996; **263**: 545–550.
9. Guldi DM, Torres-Garcia G, Mattay J. *J. Phys. Chem. A* 1998; **102**: 9679–9685.
10. Larsson S, Klimkans A, Rodriguez-Monge L, Duskesas G. *J. Mol. Struct.* 1998; **425**: 155–159.
11. Bahr JL, Kuciauskas D, Liddell PA, Moore AL, Moore TA, Gust D. *J. Photochem. Photobiol.* 2000; **72**: 598–611.
12. Kuciauskas D, Liddell PA, Lin S, Stone S, Moore AL, Moore TA, Gust D. *J. Phys. Chem. B* 2000; **104**: 4307–4321.
13. Liddell PA, Kuciauskas D, Sumida JP, Nash B, Nguyen D, Moore AL, Moore TA, Gust D. *J. Am. Chem. Soc.* 1997; **119**: 1400–1405.
14. Gust D, Moore TA, Moore AL, Liddell PA, Kuciauskas D, Sumida JP, Nash B, Nguyen D. In *Recent Advances in the Chemistry and Physics of Fullerenes and Related Materials*, Kadish KM, Rutherford AW (eds). Electrochemical Society: Pennington, NJ, 1997; 9–24.
15. Gust D, Moore TA, Moore AL, Kuciauskas D, Liddell PA, Halbert BD. *J. Photochem. Photobiol. B* 1998; **43**: 209–216.
16. Kuciauskas D, Liddell PA, Moore TA, Moore AL, Gust D. In *Recent Advances in the Chemistry and Physics of Fullerenes and Related Materials*, Kadish KM, Ruoff RS (eds). Electrochemical Society: Pennington, NJ, 1998; 242–261.
17. Kuciauskas D, Liddell PA, Moore AL, Moore TA, Gust D. *J. Am. Chem. Soc.* 1998; **120**: 10880–10886.
18. Gust D, Moore TA, Moore AL. *Acc. Chem. Res.* 2001; **34**: 40–48.
19. Carbonera D, Di Valentin M, Corvaja C, Agostini G, Giacometti G, Liddell PA, Kuciauskas D, Moore AL, Moore TA, Gust D. *J. Am. Chem. Soc.* 1998; **120**: 4398–4405.
20. Smirnov SN, Liddell PA, Vlassiouk IN, Teslja A, Kuciauskas D, Otero L, Braun CL, Moore AL, Moore TA, Gust D. *J. Phys. Chem.* 2003; **107**: 7567–7573.
21. Littler BJ, Ciringh Y, Lindsey JS. *J. Org. Chem.* 1999; **64**: 2864–2872.
22. Lee C-H, Lindsey JS. *Tetrahedron* 1994; **50**: 11427–11440.
23. Gust D, Moore TA, Luttrull DK, Seely GR, Bittersmann E, Bensasson RV, Rougée M, Land EJ, de Schryver FC, Van der Auweraer M. *Photochem. Photobiol.* 1990; **51**: 419–426.
24. Davis FS, Nemeth GA, Anjo DM, Makings LR, Gust D, Moore TA. *Rev. Sci. Instrum.* 1987; **58**: 1629–1631.
25. Freiberg A, Timpmann K, Lin S, Woodbury NW. *J. Phys. Chem. B* 1998; **102**: 10974–10982.
26. Golub GH, Reinsch C. *Numer. Math.* 1970; **14**: 403–420.
27. Henry ER, Hofrichter J. *Methods in Enzymol.* 1999; **210**: 129–192.
28. Liddell PA, Kodis G, de la Garza L, Bahr JL, Moore AL, Moore TA, Gust D. *Helv. Chim. Acta* 2001; **84**: 2765–2783.
29. Gust D, Moore TA, Moore AL, Liddell PA. *Methods Enzymol.* 1992; **213**: 87–100.
30. Kodis G, Liddell PA, de la Garza L, Moore AL, Moore TA, Gust D. *J. Mater. Chem.* 2002; **12**: 2100–2108.
31. Imahori H, Cardoso SL, Tatman D, Lin S, Macpherson AN, Noss L, Seely GR, Sereno L, Chessa de Silber J, Moore TA, Moore AL, Gust D. *Photochem. Photobiol.* 1995; **62**: 1009–1014.
32. Gust D, Moore TA, Moore AL, Devadoss C, Liddell PA, Hermant RM, Nieman RA, Demanche LJ, DeGraziano JM, Gouni I. *J. Am. Chem. Soc.* 1992; **114**: 3590–3603.
33. Moore TA, Moore AL, Gust D. *Adv. Photosynth.* 1999; **8**: 327–339.
34. Cardoso SL, Nicodem D, Moore AL, Moore TA, Gust D. *J. Braz. Chem. Soc.* 1996; **7**: 19–29.
35. Hermant RM, Liddell PA, Lin S, Alden RG, Kang H-K, Moore AL, Moore TA, Gust D. *J. Am. Chem. Soc.* 1993; **115**: 2080–2081.
36. Fungo F, Otero L, Durantini EN, Thompson WF, Silber JJ, Moore TA, Moore AL, Gust D, Sereno L. *Phys. Chem. Chem. Phys.* 2003; **5**: 469–475.
37. Bensasson RV, Land EJ, Truscott TG. *Flash Photolysis and Pulse Radiolysis: Contributions to the Chemistry of Biology and Medicine*. Pergamon: New York, 1983; 1–19.
38. Dutton PL, Leigh JS, Seibert M. *Biochem. Biophys. Res. Commun.* 1972; **46**: 406–413.
39. Thurnauer MC, Katz JJ, Norris JR. *Proc. Natl Acad. Sci. USA* 1975; **72**: 3270–3274.
40. Frank HA, Machnicki J, Friesner RA. *Photochem. Photobiol.* 1983; **38**: 451–455.
41. Levanon H, Norris JR. *Chem. Rev.* 1978; **78**: 185–198.
42. Parson WW, Clayton RK, Cogdell RJ. *Biochim. Biophys. Acta* 1975; **387**: 265–278.
43. Schenck CC, Mathis P, Lutz M. *Photochem. Photobiol.* 1984; **39**: 407–417.
44. Marcus RA. *J. Chem. Phys.* 1956; **24**: 966–978.
45. Marcus RA, Sutin N. *Biochim. Biophys. Acta* 1985; **811**: 265–322.
46. Hush NS. *J. Chem. Phys.* 1958; **28**: 962–972.
47. Hush NS. *Trans. Faraday Soc.* 1961; **57**: 557–580.
48. Kuciauskas D, Liddell PA, Hung S-C, Lin S, Stone S, Seely GR, Moore AL, Moore TA, Gust D. *J. Phys. Chem.* 1997; **101**: 429–440.
49. Noss L, Liddell PA, Moore AL, Moore TA, Gust D. *J. Phys. Chem. B* 1997; **101**: 458–465.
50. Strachan JP, Gentemann S, Seth J, Kalsbeck WA, Lindsey JS, Holten D, Bocian DF. *J. Am. Chem. Soc.* 1997; **119**: 11191–11201.

51. Yang SI, Seth J, Balasubramanian T, Kim D, Lindsey JS, Holten D, Bocian DF. *J. Am. Chem. Soc.* 1999; **121**: 4008–4018.
52. Yang SI, Seth J, Strachan JP, Gentemann S, Kim D, Holten D, Lindsey JS, Bocian DF. *J. Porphyrins Phthalocyanines* 1999; **3**: 117–147.
53. Kuciauskas D, Liddell PA, Lin S, Johnson TE, Weghorn SJ, Lindsey JS, Moore AL, Moore TA, Gust D. *J. Am. Chem. Soc.* 1999; **121**: 8604–8614.
54. Kodis G, Liddell PA, de la Garza L, Clausen PC, Lindsey JS, Moore AL, Moore TA, Gust D. *J. Phys. Chem. A* 2002; **106**: 2036–2048.
55. Jayaraj K, Gold A, Austin RN, Ball LM, Terner J, Mandon D, Weiss R, Fischer J, DeCian A, Bill E, Muether M, Schuenemann V, Trautwein AX. *Inorg. Chem.* 1997; **36**: 4555–4566.
56. Hariprasad G, Dahal S, Maiya BG. *J. Chem. Soc., Dalton Trans.* 1996; 3429–3436.
57. Gust D, Moore TA, Makings LR, Liddell PA, Nemeth GA, Moore AL. *J. Am. Chem. Soc.* 1986; **108**: 8028–8031.
58. Osuka A, Yamada H, Shinoda T, Nozaki K, Ohno O. *Chem. Phys. Lett.* 1995; **238**: 37–41.